


# Varicella zoster virus-induced autophagy in human neuronal and hematopoietic cells exerts antiviral activity

Johanna L. Heinz<sup>1,2</sup> | Daniëla M. Hinke<sup>1,2</sup> | Muyesier Maimaitili<sup>1</sup> | Jiayi Wang<sup>3</sup> |  
Ira K. D. Sabli<sup>4,5</sup> | Michelle Thomsen<sup>1,2</sup> | Ensieh Farahani<sup>1</sup> | Fanghui Ren<sup>1</sup> |  
Lili Hu<sup>1,2</sup> | Thomas Zillinger<sup>1,6</sup> | Anna Grahn<sup>7</sup> | Joanna von Hofsten<sup>8,9</sup> |  
Georges M. G. M. Verjans<sup>10</sup> | Søren R. Paludan<sup>1</sup> | Abel Viejo-Borbolla<sup>3,11</sup>  |  
Vanessa Sancho-Shimizu<sup>4,5</sup> | Trine H. Mogensen<sup>1,2</sup>

<sup>1</sup>Department of Biomedicine, Aarhus University, Aarhus, Denmark

<sup>2</sup>Department of Infectious Diseases, Aarhus University Hospital, Aarhus, Denmark

<sup>3</sup>Institute of Virology, Hannover Medical School, Hannover, Germany

<sup>4</sup>Dept of Paediatric Infectious Diseases & Virology, Imperial College London, London, UK

<sup>5</sup>Centre for Paediatrics and Child Health, Imperial College London, London, UK

<sup>6</sup>Institute of Clinical Chemistry and Clinical Pharmacology, Medical Faculty, University Hospital Bonn, Bonn, Germany

<sup>7</sup>Department of Infectious Diseases, Institute of Biomedicine, The Sahlgrenska Academy at University of Gothenburg, Gothenburg, Sweden

<sup>8</sup>Department of Clinical Neuroscience, Institute of Neuroscience and Physiology, Sahlgrenska Academy, University of Gothenburg, Gothenburg, Sweden

<sup>9</sup>Department of Ophthalmology, Halland Hospital Halmstad, Halmstad, Sweden

<sup>10</sup>Department of Viroscience, HerpeslabNL, Erasmus University MC, Rotterdam, The Netherlands

<sup>11</sup>Cluster of Excellence-Resolving Infection Susceptibility (RESIST, EXC 2155), Hannover Medical School, Hannover, Germany

## Correspondence

Trine H. Mogensen, Department of Biomedicine, Aarhus University, Aarhus, Denmark.  
Email: [trine.mogensen@biomed.au.dk](mailto:trine.mogensen@biomed.au.dk) and [trinmoge@rm.dk](mailto:trinmoge@rm.dk)

## Funding information

Danmarks Frie Forskningsfond, Grant/Award Number: 4004-00047B; Novo Nordisk research foundation, Grant/Award Numbers: NNF21OC0067157, NNF20OC0063436; Danmarks Grundforskningsfond, Grant/Award Number: DNRF164; Lundbeck Foundation, Grant/Award Number: R268-3927;

## Abstract

Autophagy is a degradational pathway with pivotal roles in cellular homeostasis and survival, including protection of neurons in the central nervous system (CNS). The significance of autophagy as antiviral defense mechanism is recognized and some viruses hijack and modulate this process to their advantage in certain cell types. Here, we present data demonstrating that the human neurotropic herpesvirus varicella zoster virus (VZV) induces autophagy in human SH-SY5Y neuronal cells, in which the pathway exerts antiviral activity. Productively VZV-infected SH-SY5Y cells showed increased LC3-I-LC3-II conversion as well as co-localization of the viral glycoprotein E and the autophagy receptor p62. The activation of autophagy was

**Abbreviations:** AIM, absent in melanoma; ARN, acute retinal necrosis; BSA, bovine serum albumin; CADD, combined annotation dependent depletion; CNS, central nervous system; CSF, colony stimulating factor 1; CQ, Chloroquine; DAPI, 4',6-diamidino-2-phenylindole; DMEM, Dulbecco's Modified Eagle Medium; EBSS, Earle's Balanced Salt Solution; ER, endoplasmic reticulum; FBS, fetal bovine serum; g, glycoprotein; HBSS, Hanks' Balanced Salt Solution; hESC, Human embryonic stem cells; HI, heat inactivated; HSE, herpes simplex encephalitis; HSV, herpes simplex virus; IEL, inborn errors of immunity; IFN, interferon; iPSC, induced pluripotent stem cells; KD, knock-down; M-CSF, macrophage colony stimulating factor; MdMs, monocyte derived macrophages; MOI, multiplicity of infection; MSC, mutation significance cutoff; NF- $\kappa$ B, nuclear factor kappa-light-chain-enhancer of activated B; NLRP, nucleotide-binding oligomerization domain; P1/2, Patient 1/2; PBMC, peripheral blood mononuclear cells; PBS, phosphate-buffered saline; PCR, polymerase chain reaction; RPMI, Roswell Park Memorial Institute; TCID<sub>50</sub>, 50% tissue culture infectious dose; VZV, varicella zoster virus; WES, whole exome sequencing.

This is an open access article under the terms of the [Creative Commons Attribution-NonCommercial-NoDerivs](https://creativecommons.org/licenses/by-nc-nd/4.0/) License, which permits use and distribution in any medium, provided the original work is properly cited, the use is non-commercial and no modifications or adaptations are made.

© 2024 The Author(s). *Journal of Medical Virology* published by Wiley Periodicals LLC.

The German Research Council (DRG),  
Grant/Award Number: 390874280; JLH  
received support from Danielsens Fond

dependent on a functional viral genome. Interestingly, inducers of autophagy reduced viral transcription, whereas inhibition of autophagy increased viral transcript expression. Finally, the genotype of patients with severe ocular and brain VZV infection were analyzed to identify potential autophagy-associated inborn errors of immunity. Two patients expressing genetic variants in the autophagy genes *ULK1* and *MAP1LC3B2*, respectively, were identified. Notably, cells of both patients showed reduced autophagy, alongside enhanced viral replication and death of VZV-infected cells. In conclusion, these results demonstrate a neuro-protective role for autophagy in the context of VZV infection and suggest that failure to mount an autophagy response is a potential predisposing factor for development of severe VZV disease.

#### KEYWORDS

acute retinal necrosis, autophagy, CNS infection, innate immunity, varicella zoster virus

## 1 | INTRODUCTION

Autophagy has been recognized as a degradational pathway serving to maintain homeostasis in eukaryotic cells for more than 60 years.<sup>1,2</sup> Cytoplasmic contents are sequestered during macro-autophagy; hereupon referred to as autophagy. Its longstanding conservation throughout evolution underscores the immense importance of autophagy for survival of cells and organisms.<sup>3–5</sup> In the autophagy process, intracellular cargo is marked for degradation and subsequently enclosed within a double-membraned phagophore. Upon completion of the autophagosome the cargo is broken down in the context of fusion with lysosomes by increased acidification and enzymatic degradation.<sup>6–8</sup> The rate of autophagic activity is defined by formation of autophagosomes and their subsequent degradation is referred to as autophagic flux.<sup>9</sup> Additionally, autophagosomes are able to fuse with endosomes, leading either to digestion of the cargo or transport to the plasma membrane for exocytosis of its contents.<sup>10–13</sup>

While basal autophagy serves to maintain homeostasis through recycling of organelles and proteins,<sup>14</sup> the pathway is further upregulated during conditions of stress- and starvation.<sup>15–17</sup> Importantly, accumulating evidence shows an essential role of autophagy in response to infection with a range of different pathogens.<sup>18–21</sup> Autophagy can exert antiviral activity in numerous ways, for example by directly degrading viral particles (xenophagy), by activating innate immune responses, and by promoting major histocompatibility complex class I and II antigen presentation.<sup>22</sup> On the other hand, autophagy can negatively regulate inflammation by degrading inflammasome components, such as nucleotide-binding oligomerization domain (NLRP)3 and absent in melanoma (AIM)2, and by counteracting the interferon (IFN) response and the nuclear factor kappa-light-chain-enhancer of activated B cells (NF- $\kappa$ B) pathway.<sup>23–25</sup> Moreover, some viruses have adapted to evade digestion and instead utilize autophagic vesicles as a means to replicate and exit the cell.<sup>26–30</sup>

VZV is a pathogen of the  $\alpha$ -herpesvirus subfamily and has been described to induce autophagy upon infection.<sup>31</sup> Unlike the closely related herpes simplex virus (HSV)-1 and HSV-2, VZV does not encode for any proteins interfering with autophagy; hence, complete autophagic flux has been observed in VZV infected fibroblasts and melanoma cells.<sup>32</sup> Moreover, VZV has been proposed to benefit from complete autophagy, at least in fibroblasts, potentially exploiting the pathway to egress from infected cells.<sup>33</sup> The clinical phenotype of primary infection with VZV is varicella (chickenpox). A hallmark of herpesvirus infection is the establishment of latency in the host succeeding primary infection, in the case of VZV mainly in sensory dorsal root and trigeminal ganglia.<sup>34,35</sup> Depending on the immunity of the host, the virus may reactivate decades later in an estimated 1 of 3 infected individuals, giving rise to zoster.<sup>36,37</sup> In rare cases severe complications can arise after either primary infection or reactivation, with involvement of the CNS, potentially, including VZV meningitis, encephalitis, or acute retinal necrosis (ARN).<sup>38–41</sup> VZV encephalitis occurs in an estimated 1 out of 10 000 infected individuals and can manifest as a stroke-like presentation due to vasculitis of large- and small vessels in both immunocompromised and immunocompetent individuals. VZV encephalitis may lead to permanent sequelae, including cognitive impairment and memory loss.<sup>42</sup> Likewise, ARN is a rare ocular disease manifestation only occurring with an incidence of 1 out of 2 million individuals every year.<sup>41</sup> Nonetheless, the consequences of this retinal inflammation can be serious, and in the worst-case result in permanent loss of vision.<sup>43</sup> Severe complications of VZV infection are most commonly observed in immunocompromised individuals or those having reached the age of immunosenescence, whereas occurrence in young, otherwise healthy individuals may suggest an underlying inborn error of immunity (IEI).<sup>44–46</sup>

The aim of the current study was to determine the role of autophagy in antiviral defence against VZV in human neuronal cell types and a potential pathogenic role for defective autophagy in predisposing to VZV pathologies in the CNS in humans. We show that VZV infection of neuronal cells induces autophagy and that

impaired autophagy results in enhanced viral replication, whereas autophagy-inducing agents decrease viral titres. Further, we describe the identification and characterization of variants in genes encoding essential autophagy molecules, including *ULK1* in a VZV encephalitis patient (P1) and *MAP1LC3B2* in a VZV ARN patient (P2). Cells from these patients show reduced autophagy in response to VZV infection alongside elevated VZV replication and enhanced cell death.

## 2 | METHODS

Methods are described in greater detail in supplementary methods.

### 2.1 | Patient inclusion & material

P1 was included as P1 in a VZV encephalitis cohort described by Thomsen et al. (2021),<sup>47</sup> and P2 was included as P2 in an ARN cohort described by Heinz et al. (2023).<sup>48</sup> Whole blood was collected into EDTA tubes for DNA extraction and in lithium heparin tubes for peripheral blood mononuclear cell (PBMC) isolation.

### 2.2 | WES & bioinformatics

DNA was extracted from whole blood and subjected to WES at the Department of Molecular Medicine, Aarhus University Hospital, and subsequently analyzed in Ingenuity Variant Analysis (IVA, Qiagen, Hilden, Germany).<sup>49,50</sup>

### 2.3 | STRING analysis

The protein interactome for human *ULK1* and *LC3B2* was obtained using the STRING analysis software (version 11.5; STRING Consortium 2023<sup>51</sup>), medium confidence (0.400). All shown nodes are query proteins and first shell of interactors. The graphics was subsequently modified in Adobe Illustrator 2023.

### 2.4 | Popviz

The PopViz plot<sup>52</sup> was generated using PopViz webserver (<https://hgidsoft.rockefeller.edu/PopViz/>) and further modified in Adobe Illustrator 2023

### 2.5 | Conservation analysis

Protein sequences for *ULK1* and *LC3B2* in different species were aligned using the NCBI webserver (<https://www.ncbi.nlm.nih.gov/tools/cobalt/cobalt.cgi?CMD=Web>) and modified using Adobe Illustrator 2023.

### 2.6 | Cell culture, viral infections and stimulations

PBMCs were isolated from whole blood by Ficoll density gradient centrifugation using SepMate PBMC isolation tubes (Stemcell Technologies, Vancouver, Canada) as described before<sup>53</sup> and cultured in Roswell Park Memorial Institute (RPMI)-1640 medium (cat# L0500, VWR, Radnor, Pennsylvania) supplemented with 10% heat-inactivated fetal bovine serum (FBS) (cat# S181H, Biowest, Nuaille, France), 100 IU/ml penicillin, and 100 µg/ml streptomycin (1% P/S) (cat# 15-140-122, Thermo Fisher Scientific, Waltham, Massachusetts). Monocyte derived macrophages (MdmMs) were isolated from  $5 \times 10^5$  patient and control PBMCs. The human neuroblastoma cell line SH-SY5Y (ATCC, CRL-2266) was grown in Dulbecco's Modified Eagle Medium (DMEM) high glucose (cat# L0102, Biowest, Nuaille, France) supplemented with 10% HI FBS and 1% P/S. Uninfected or VZV infected human malignant melanoma MeWo (ATCC, HTB-65) cells were cultured in DMEM high glucose supplemented with 10% HI FBS and 1% P/S. Cells were infected with cell-free isolates<sup>54</sup> of VZV recombinant Oka strain = rOka strain (ATCC, VR-1832), the clinical isolate VZV EMC-1 or MeWo-associated VZV rOka/pOka or treated with stimuli indicated in the regarding figure and supplementary methods.<sup>55</sup>

### 2.7 | Differentiation of SH-SY5Y cells

Was done as previously described and further detailed in supplementary methods.<sup>56</sup>

### 2.8 | Generation of hESC-derived neurons

Was done as previously described and further detailed in supplementary methods.<sup>55,57</sup>

### 2.9 | Generation of knock-downs and knock-ins in SH-SY5Y cells

Knock-down (KD) cell lines were generated by nucleofection with a CRISPR-Cas9 system following the manufacturer's instructions using the Amaxa 4D-Nucleofector protocol for SH-SY5Y cells (Lonza Cologne GmbH). gRNA AAVS1: GGGGCCACUAGGGACAGGAU, U LK1::GUCCUCGUCAGCGUGCGCA, LC3B2: UUCAAGCAGCGCCG-CACCUU, ATG5: AAAAAGAUCACAAGCAACUC.

Knock-in single cell clones of the patient variant in *LC3B2* were generated using the same system. gRNA LC3B2: GTGCCTCCAG-GAGACGTTT, HDR-template: GAGAGTGAGAAAGATGAAGATG-GATTCCTGTACATGGTCTGcGcCaTCCCAGGAGACcTTCaGaAT-GAAATTGTCAGTGATAAACCGAAAAAATGCATCTCTTCTA-GAATTTTTTAAACC. Following, single cell clones harbouring the patient variant in a heterozygous manner were selected.

## 2.10 | Immunoblotting

Western blots were carried out as described previously<sup>58</sup> and in supplementary methods.

## 2.11 | RNA and DNA isolation & qRT-PCR

Total RNA was purified using Nucleospin 96 RNA core kit (cat# 740466.4, Macherey-Nagel, Düren, Germany) and subsequently reverse-transcribed into cDNA using Iscript™ gDNA Clear cDNA Synthesis Kit (cat# 1725035, Bio-Rad, Hercules, CA). Genomic DNA was purified using GeneJET DNA Purification Kit (cat# K0722, Thermo Fisher Scientific). Following, mRNA and gDNA expression was measured by RT-qPCR, as indicated in the regarding figures and supplementary methods.

## 2.12 | Immunofluorescence staining

SH-SY5Y cells were subsequently to treatments fixed with 4% paraformaldehyde (cat# 47608, Merck, Rahway, New Jersey), permeabilized using 100% ice cold methanol (cat# 67-56-1, Merck, Rahway, New Jersey), blocked 1 h on RT in 10% FBS in PBS and then stained for targets indicated in the regarding figures and supplementary methods.<sup>59-62</sup>

## 2.13 | AnnexinV staining

PBMCs were stimulated, harvested, blocked with human TruStain FcX TM (cat# 422302, Biolegend, San Diego, California, 5  $\mu$ L/well) in 45  $\mu$ L flow staining buffer (1% FBS in PBS) per well for 10 min and stained for cell surface markers, as indicated in supplementary methods. Cells were analyzed using a Novocyte Quanteon 4025, Agilent (Santa Clara, California) and FlowJo software version 10.9.0 (BD Biosciences, Franklin Lakes, New Jersey).

## 2.14 | Statistics

Experiments were performed in biological triplicates. Unpaired t-tests/one/two-way ANNOVA was performed as indicated for the individual experiments utilizing GraphPad Prism 10.1.

# 3 | RESULTS

## 3.1 | VZV infection of human neuronal cell lines and monocyte-derived macrophages induces autophagy

To evaluate the role of autophagy in VZV-infected cell types relevant to severe VZV CNS infection, we tested the ability of

VZV to induce LC3-I to LC3-II conversion in the human neuroblastoma cell line SH-SY5Y.<sup>9</sup> As a means of measuring autophagic flux, we also compared LC3-I to LC3-II conversion in the presence or absence of the late stage autophagy inhibitor chloroquine (CQ).<sup>9</sup> LC3-I to LC3-II conversion was significantly increased at 72 hpi in SH-SY5Y neuronal cells infected with the cell-free clinical VZV isolate EMC-1 at a multiplicity of infection (MOI) of 0.1 (Figure 1A,B). Importantly, VZV-induced autophagy flux was enhanced as demonstrated by significantly elevated LC3-I to LC3-II conversion in virus-infected cells in the presence of chloroquine (Figure 1A,B). Moreover SH-SY5Y cells infected with the cell-free VZV pOka strain also showed LC3-I to LC3-II conversion, although this did not reach statistical significance, except for LC3-I to LC3-II conversion by pOka in the absence of chloroquine (Fig. S1A,B). The data suggest that VZV infection induces initiation of early-stage autophagy and/or blocking of late-stage autophagy in SH-SY5Y cells. The MeWo cells used for generating cell-associated VZV showed high basal levels of LC3-I to LC3-II conversion leading to increased LC3-II/LC3-I ratios in mock-infected SH-SY5Y cells and consequently were not used for further experiments in this study (Fig. S1C). Next, ultraviolet light (UV)-inactivation of VZV EMC-1 greatly diminished glycoprotein (g)E expression and LC3-I to LC3-II conversion, demonstrating that autophagy induction by VZV requires a functional, replicating genome and may be triggered by a late viral product or general cellular stress caused by viral replication (Figure 1C,D and Fig S1D,E).

To confirm these observations in cell types resembling neurons to a higher degree, we performed similar experiments in mature human neurons differentiated from SH-SY5Y neuroblastoma cells<sup>56</sup> (Figure 1E,F) and from human embryonic stem cells (hESC)<sup>55,57</sup> (Figure 1G,H). Importantly, both differentiated neuronal cell types exhibited neuron-like morphology (Fig. S1D,E). Infecting these neuronal cells, we observed the same phenomenon of VZV-induced LC3-I to LC3-II conversion, albeit to a lower degree and not reaching statistical significance (Figure 1E,F,G,H). EBSS largely did not induce autophagy in this cell type. Based on these data, hypothesize that autophagy induction is a general mechanism in VZV-infected neurons and neuronal-like cell types. Infection of these cells was confirmed by expression of VZV gE (Figure 1E,G), expression of VZV *ORF63*, *ORF9*, and *ORF40* mRNA (Fig. S1F-H) as well as from production of VZV genomic *ORF63* DNA (Fig. S1I). Finally, as an additional cell type with high basal autophagy and relevant to the immune response against VZV, we also tested the effect of VZV infection in MdMs.<sup>63,64</sup> We detected increased LC3-I to LC3-II conversion in response to cell-free VZV rOka at 48 hpi, which was enhanced by the presence of CQ (Figure 1I,J), suggesting uninterrupted autophagy flux upon VZV infection. In this cell type EBSS is largely not inducing autophagy. Taken together, these results show activation of autophagy after VZV infection in different human cell types relevant for VZV pathogenesis.

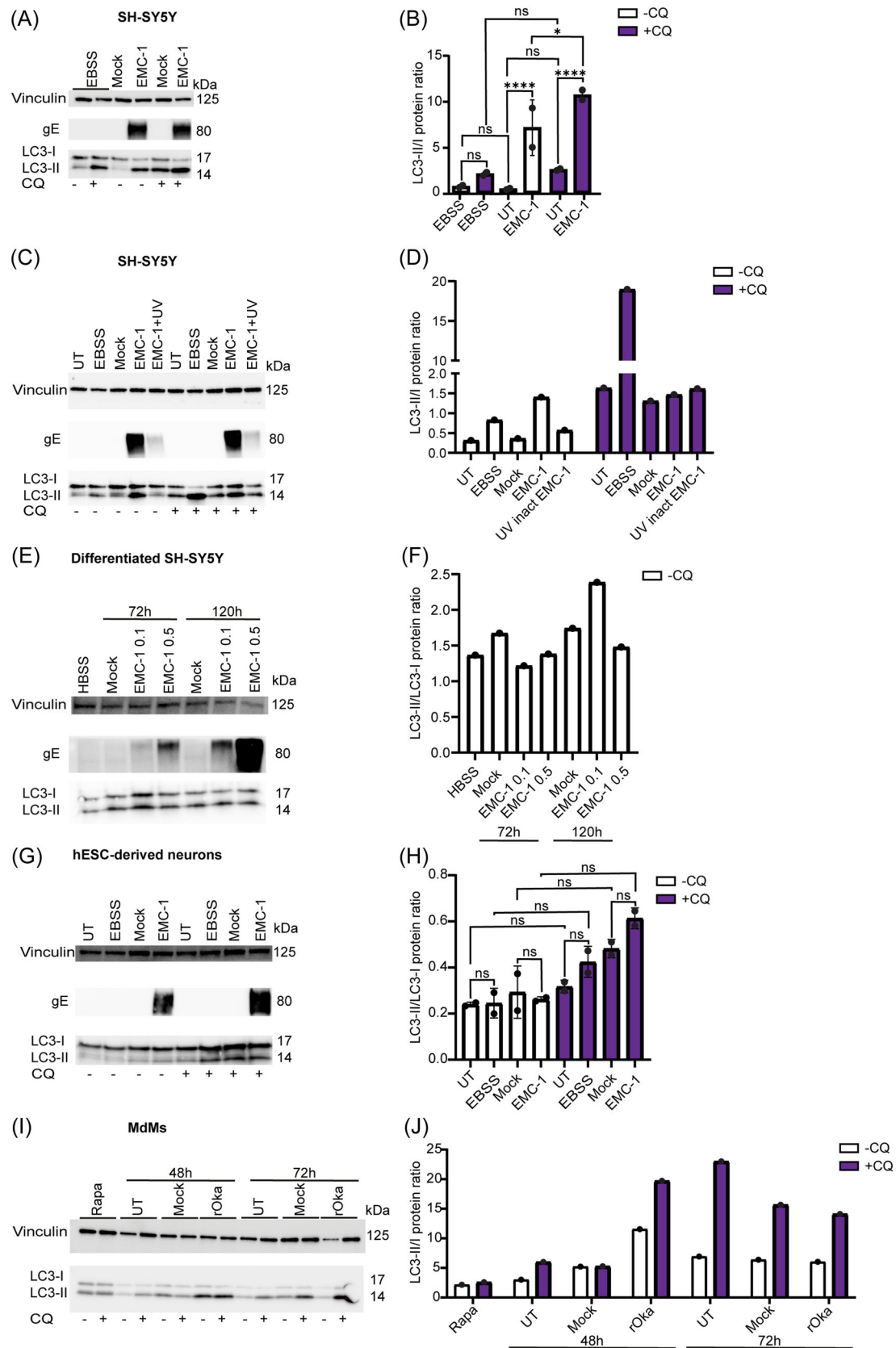


**FIGURE 1** (See caption on next page).

### 3.2 | VZV glycoprotein E co-localizes with the autophagy receptor p62

To further characterize the mechanism and kinetics of VZV-induced autophagy, we analyzed SH-SY5Y neuroblastoma cells infected with cell-free VZV EMC-1 by immunofluorescence (Figure 2). First, VZV gE was detectable in VZV-infected cells, although lack of gE does not necessarily exclude some degree of infection (Figure 2A-C). VZV infection led to an increase in LC3 punctae in cells, both where gE was visible and where this signal was not detectable by the methodology used (Figure 2A and D). Most strikingly though, VZV EMC-1 infection led to higher p62 intensities in the cytoplasm of productively infected cells, exhibiting a punctate staining pattern (Figure 2A,B and E). Moreover, the autophagy cargo receptor p62 colocalized with VZV gE. Pearson's correlation coefficient is commonly used to quantify co-localization by comparing fluorescence intensities at every pixel of an image for two channels.<sup>65</sup> Values > 0.5 indicate strong co-localization, whereas values < 0.5 but > 0.3 medium correlation. The mean Pearson correlation coefficient for p62 and gE was 0.35 (Figure 2F). Further, Mander's overlap coefficient is able to differentiate between the fractions of p62 that co-localize with gE and vice versa. Again, values > 0.5 suggest a high level of colocalization.<sup>65,66</sup> When comparing Mander's overlap coefficients for the fractions of gE overlapping with p62 (Mander's coefficient 1, Figure, 2G) and the fractions of p62 overlapping with gE (Mander's coefficient 2, Figure 2H) it becomes apparent that a large fraction of gE overlapped with p62, whereas a much smaller portion of total p62 coincided with gE. This might be interpreted as recruitment of p62 to viral gE. In summary, these results corroborate with the immunoblot data, supporting the conclusion that VZV activates autophagy in SH-SY5Y cells and demonstrate co-localization of viral proteins with autophagosomes.

### 3.3 | Activation of autophagy inhibits VZV gene transcription

Following the observation that VZV activates autophagy, we sought to determine whether autophagy exerts a pro- or antiviral role in the

neuronal cells. To this end we treated cells with ML288, a compound that activates hypoxia-inducible factor, which in turn induces autophagy. ML288 was recently identified to exert antiviral activity in SH-SY5Y cells against HSV-1 and 2 in a manner dependent on autophagy.<sup>55</sup> We confirmed the autophagy-inducing activity of ML288 (Figure 3A and B). SH-SY5Y cells pretreated with ML288 for 2 h were infected with VZV rOka (MOI 0.005) or EMC-1 (MOI 0.01), according to optimization experiments showing optimal infection at these MOIs for the different VZV strains. Notably, ML288 pretreatment significantly lowered the transcription of the analyzed VZV ORFs (Figure 3C-H). ORF9 encodes for a tegument protein with early-late expression kinetics,<sup>67,68</sup> ORF40 for a late expressed nucleocapsid protein<sup>69</sup> and ORF63 for a viral transcription factor with immediate early kinetics.<sup>70</sup> Measurement of viral ORFs is a common approach to estimate VZV replication, as the extreme cell-associated nature of the virus complicates the use of classical replication assays, such as plaque assay or 50% tissue culture infectious dose (TCID<sub>50</sub>).<sup>71</sup> These data demonstrate that that autophagy serves an antiviral function in the neuroblastoma cell line SH-SY5Y.

### 3.4 | Neuronal cells deficient in essential autophagy proteins support increased VZV gene expression

To build onto the previous results, we aimed to block autophagy by knocking down expression of relevant, essential autophagy-related genes in SH-SY5Y neuroblastoma cells (Fig. S2A). For this purpose, we chose ATG5, a well described protein essential for functioning autophagy, as well as ULK1 and LC3B2, two key players in autophagy at early steps of autophagy initiation or later steps of autophagosome maturation, respectively.<sup>4,9,72</sup> AAVS1 was used for mock transfection as control. Figure 4A shows LC3-I to LC3-II conversion and p62 expression (LC3-I to LC3-II conversion shown in Fig S2B) in WT and AAVS1-depleted SH-SY5Y cells, with the strongest effect in response to VZV EMC-1 infection or EBSS starvation combined with CQ treatment. As expected, the ATG5 deficient cells exhibited a total block in LC3-I to LC3-II conversion.

**FIGURE 1** Varicella zoster virus infection of human neuronal cell lines and monocyte-derived macrophages induces LC3-I to LC3-II conversion. (A,C,E,G,I) Immunoblots for vinculin, VZV glycoprotein E (gE), LC3-I and LC3-II protein in lysates from VZV infected cells. (A) human neuroblastoma cells (SH-SY5Y) left untreated (UT), after 4 h starvation in EBSS or at 72 h postinfection (hpi) with cell-free EMC-1 MOI 0.1, or the relevant mock control, in the presence or absence of chloroquine (CQ). (C) SH-SY5Y cells left untreated, incubated for 4 h in starvation medium in EBSS or infected for 72 h with normal or UV-inactivated cell-free VZV EMC-1 MOI 0.1 in the presence or absence of CQ. Experiment shown is representative for 3 independent experiments. (E) Differentiated SH-SY5Y after 4 h starvation in EBSS or at 72 or 120 h hpi with cell-free VZV EMC-1 MOI 0.1/0.5 or the relevant mock control, (G) human embryonic stem cells (hESC) differentiated into cortical neurons at UT, after 4 h starvation in EBSS or at 120 h hpi with cell-free VZV EMC-1 MOI 0.5 or the relevant mock control in the presence or absence of CQ. (I) human monocyte-derived macrophages (Mdm) left untreated (UT), after 4 h rapamycin treatment (Rapa) at 48 and 72 hpi with cell-free VZV rOka MOI 0.1 or relevant mock control in the presence or absence of CQ. B) Quantification of LC3-II/LC3-I ratios of 2 independent experiments shown in panel A, (D) data shown in panel C, (F) data shown in panel E, (H) 2 replicates of data shown in panel G, (J) data shown in panel I. Experiment (A-J) samples of cells treated in duplicate with (+) and without (-) chloroquine (CQ). Shown are individual data points plus mean  $\pm$  SD, statistical analysis by two-way ANOVA with Šidák's multiple comparison, \* =  $p < 0.05$  and \*\*\*\* =  $p < 0.0001$ , ns = nonsignificant.

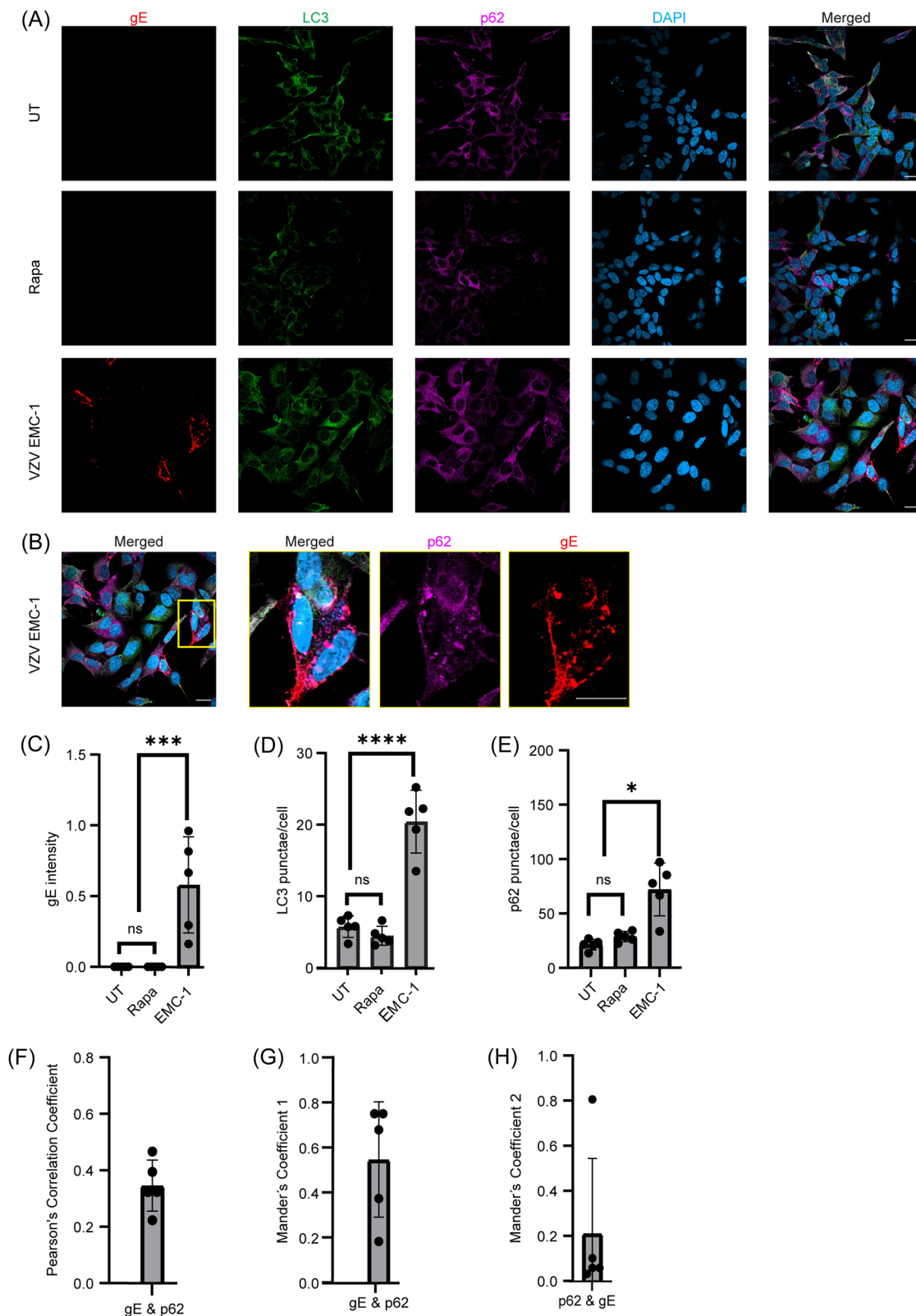


**FIGURE 2** Varicella zoster virus glycoprotein E co-localizes with the autophagy receptor p62 in a productively infected human neuronal cell line. (A and B) Immunofluorescence images of human neuroblastoma cells (SH-SY5Y) stained for VZV glycoprotein E (gE; red), LC3 (green), p62 (magenta) and DNA (DAPI; blue). Cells were mock infected (UT), treated for 24 h with rapamycin (Rapa) or infected with cell-free VZV EMC-1 strain MOI 0.2 and incubated for 48 h. Pictures are representative of 5 different images per conditions each. Scale bar = 20  $\mu$ m. (B) The box area is enlarged and shown for merged p62 and gE. (C – E) Quantification of the mean fluorescent intensity (MFI) of gE (panel C), LC3 punctae (panel D) or p62 punctae (panel E) in UT, Rapa-treated or VZV-infected human SH-SY5Y neuroblastoma cells. (F) Pearson's correlation coefficients of VZV-infected samples of data shown in panel A. (G, H) Mander's overlap coefficients for data shown in panel E (gE and p62) and F (p62 and gE). Shown are individual data points plus mean  $\pm$  SD, statistical analysis by one-way ANOVA with Dunnett's multiple comparison test, \*\* =  $p < 0.01$  and \*\*\* =  $p < 0.001$ , ns = nonsignificant.

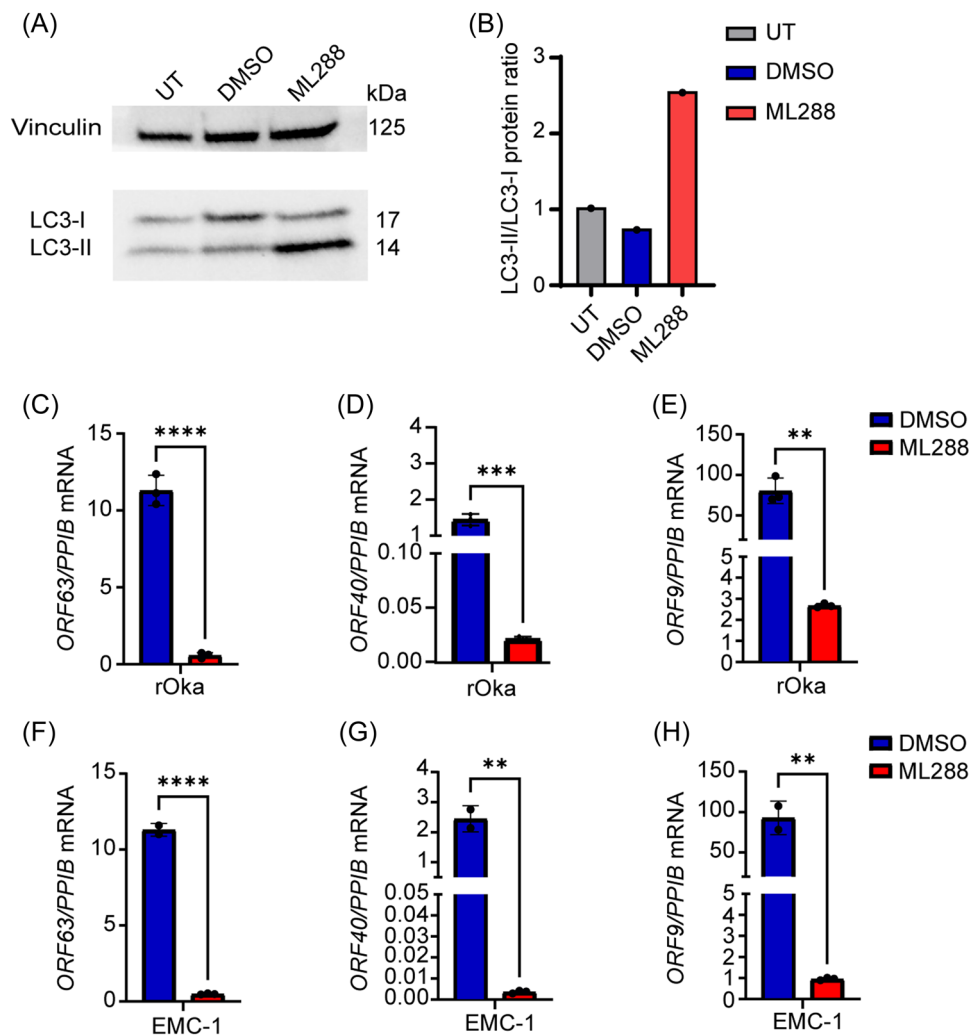


**FIGURE 3** Induction of autophagy inhibits varicella zoster virus open reading frame transcription in productively infected human neuronal cells. (A) Immunoblots for vinculin, LC3-I and LC3-II proteins in lysates from human neuroblastoma cells (SH-SY5Y) left untreated (UT) or stimulated for 50 h with the autophagy inducing compound ML288 or the vehicle control DMSO. (B) Quantification of LC3-II/LC3-I ratios shown in panel A. (C–H) relative expression of the indicated VZV open reading frames (ORF), normalized to the house keeping gene PPIB, in SH-SY5Y cells pretreated with ML288 or DMSO and subsequently productively infected with cell-free VZV rOka strain MOI 0.005 (panels C – E) or EMC-1 MOI 0.01 (panels F – H) for 48 h. Data shown are biological triplicates. Shown are individual data points plus mean  $\pm$  SD, statistical analysis by unpaired t-tests, \*\* =  $p < 0.01$ , \*\*\* =  $p < 0.001$  and \*\*\*\* =  $p < 0.0001$ , ns = nonsignificant.

In contrast, the ULK1 and LC3B2 deficient cells retained their ability to induce autophagy in response to EBSS, even though LC3B2 deficient cells showed overall decreased levels of LC3 protein (Figure 4A and S2B). We next assessed VZV transcription in these fully or partially autophagy deficient cell lines infected with rOka (Figure 4 2B-D, F-H, and J-L) or EMC1 (Fig S2C-K). These data showed increased ORF40 and ORF9 transcripts in ULK1 deficient cells and increased ORF9 transcripts in LC3B2 deficient cells compared to controls (AAVS1) infected with rOka (Figure 4C,D and H). In the context of VZV EMC-1 infection, data showed increased ORF63 and ORF9 transcripts in ULK1 deficient cells and increased ORF9 transcripts in ATG5 deficient cells compared to controls (AAVS1) (Fig S2C,E and K). To measure viral replication, we additionally analyzed viral genomic DNA levels of ORF63 in the

knock-down cell lines. Here, we observed a significant increase in ORF63 in ATG5 deficient cells infected with the EMC-1 strain compared to WT (Figure 4E,I, and M)

Immunofluorescence imaging of these cell lines with a complete or partial autophagy defect showed increased p62 and gE expression upon VZV infection (Fig S2L), which is in line with the western blot results (Figure 5A–E and S3A). Increase of p62 intensity in the cytoplasm of infected cells was only statistically significant for AAVS1-deficient, but not the autophagy knock-down cells (Figure 5A–E). Pearson's correlation coefficients for gE and p62 colocalization showed correlation in all KD cell lines (Figure 5F). Overall, these results demonstrate increased VZV ORF transcripts in SH-SY5Y cells with reduced autophagy due to defects in select autophagy genes.



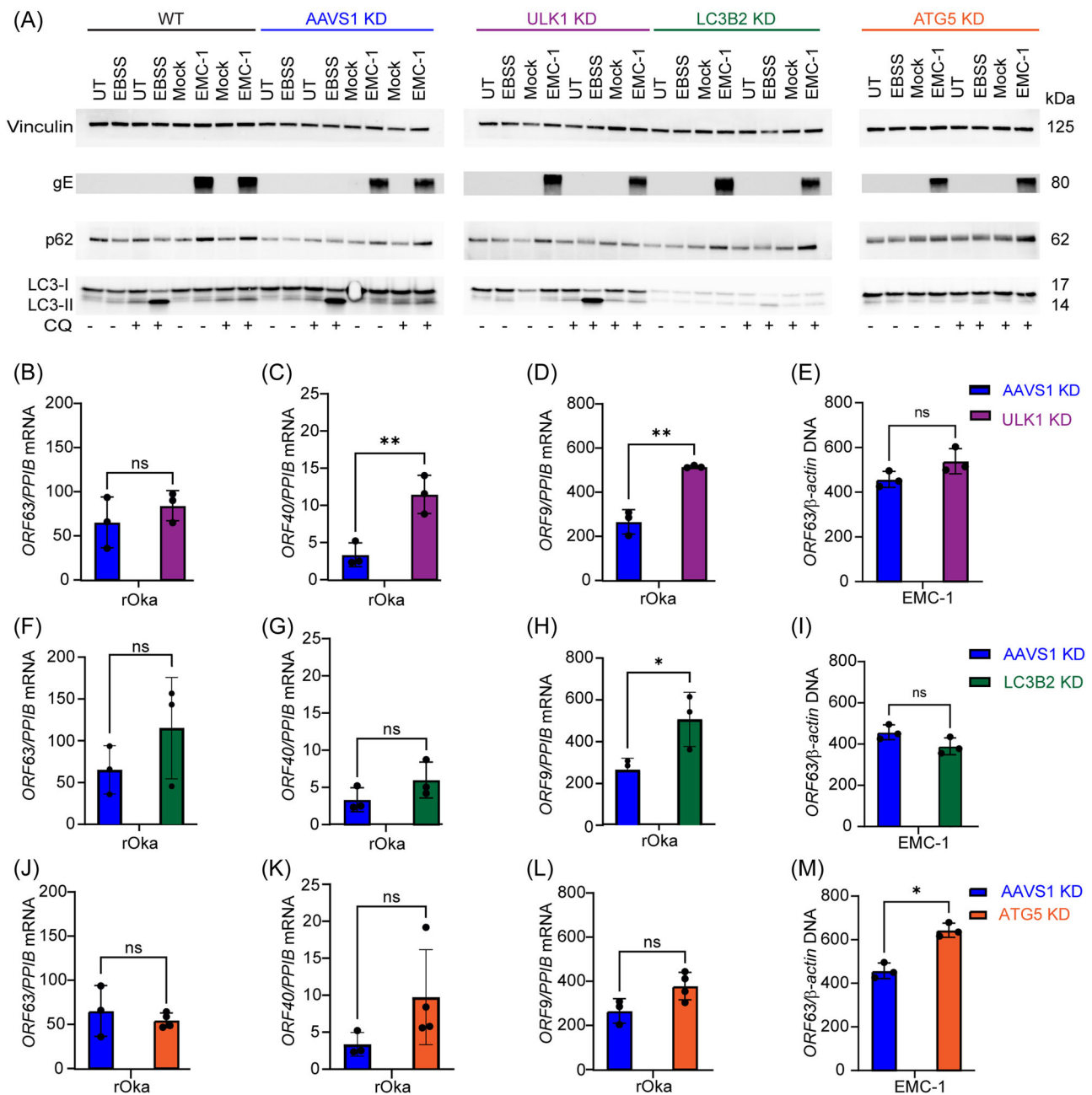


**FIGURE 4** Impaired autophagy leads to increased varicella zoster virus replication in SH-SY5Y cells. (A) Immunoblots for vinculin, VZV glycoprotein E, p62, LC3-I and LC3-II on lysates from SH-SY5Y wildtype (WT), AAVS1 knockdown (KD), ULK1 KD, LC3B2 KD, and ATG5 KD cells untreated (UT), following 4 h starvation by EBSS, infection with VZV EMC-1 strain for 72 h. All samples in duplicates +/- chloroquine (CQ). Experiment representative for 3 identical experiments. (B-D, F-H, J-L) relative mRNA expression of the indicated VZV open reading frames (ORF), normalized to the house keeping gene PPIB, in SH-SY5Y cells infected with VZV rOka MOI 5 for 72 h. 3 biological replicates per sample for AAVS1, ULK1 and LC3B2 KD, 4 biological replicates for ATG5 KD. One sample was lost in Figure 4H for AAVS1. (E, I, M) relative DNA expression of VZV ORF63 normalized to the house keeping gene  $\beta$ -actin in SH-SY5Y cells infected with VZV EMC-1 MOI 0.1. Shown are individual data points plus mean  $\pm$  SD, statistics were determined by unpaired t-tests, \* =  $p < 0.05$ , \*\* =  $p < 0.01$ , ns = nonsignificant.

### 3.5 | Identification of variants in autophagy genes in patients with severe VZV infections of the eye and brain

To pursue our findings on VZV-induced autophagy and a potential antiviral role of autophagy in neuronal cells, we asked the question

whether autophagy defects may be present in patients suffering from severe CNS infection with VZV. We therefore investigated our previously described cohorts of patients with VZV encephalitis or meningoencephalitis (N = 17)<sup>47</sup> and VZV-induced ARN (N = 17).<sup>48</sup> Bioinformatic analysis resulted in the identification of 8 variants in genes involved in the autophagy pathway in 6 of 17 (35%) VZV

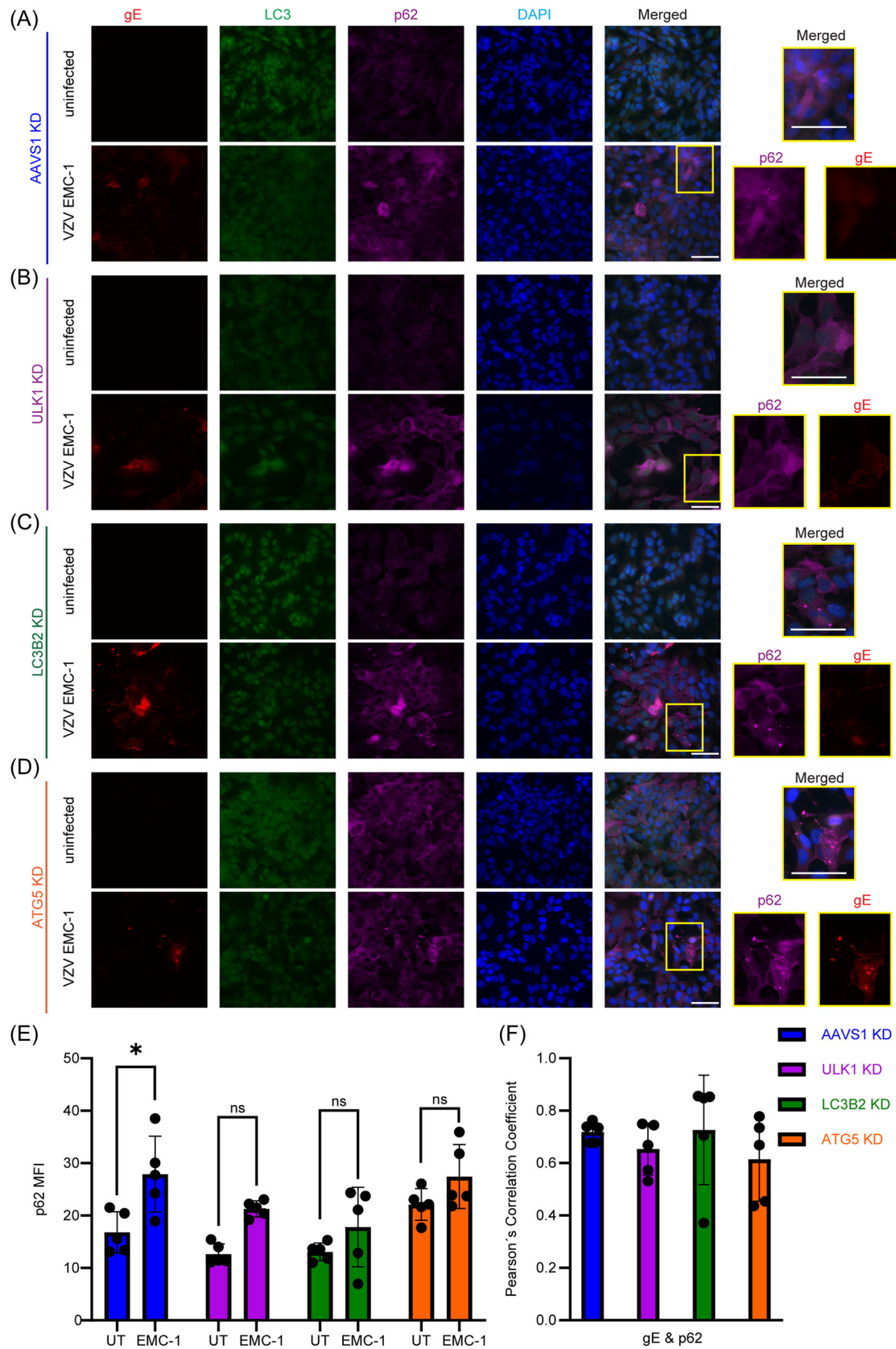


FIGURE 5 (See caption on next page).

encephalitis patients and in 6 autophagy-related variants in 7 of 17 (41%) ARN patients.<sup>47,48</sup> Based on the bioinformatic predictions on deleteriousness of these variants, combined with the central role of autophagy proteins encoded by the respective genes, we went on to functionally investigate autophagy responses and VZV replication in two of these patients. P1 is a male who developed meningoencephalitis at the age of 56 years and harbors a 1699 C > T missense variant in *ULK1*, leading to a replacement of arginine (R) to cysteine (C) at residue position 567 (R567C) (Figure 6A). R567 shows high evolutionary conservation across different species (Figure 6B), indicating the importance of this residue in *ULK1* protein function. The variant has a high CADD score of 22.7 and a low frequency in gnomAD of 0.012% (Figure 6C), suggesting a high degree of deleteriousness of this rare variant. P2, a female who developed ARN at the age of 63 years, harbors a 358 G > A missense variant in *MAP1LC3B2*, leading to a glycine (G) to arginine (R) amino acid shift at position 120 (G120R) (Figure 6A). The variant shows high conservation of the glycine at residue position 120 (Figure 6B, bottom) as well as a high CADD score of 23.2 and a low frequency of 0.03% (Figure 6D). Both *ULK1* and *LC3B2* are strongly connected to other proteins in the autophagy pathway, as revealed by STRING protein interaction network analysis (Figure 6E,F). *LC3* levels were decreased compared to controls in both patients, while *ULK1* expression was comparable to C1 but possibly higher than in C2. (Figure 6G). Additional results of the exome analysis in these VZV CNS infection cohorts is available in the respective publications.<sup>47,48</sup>

### 3.6 | Decreased levels of LC3 protein and increased VZV replication in SH-SY5Y cells harbouring the LC3B2 c.358 G > A variant identified in P2

To investigate the functional effect of the variant in *LC3B2*, an essential autophagy-related protein, in a neuronal model, we created SH-SY5Y single cell clones harbouring the *LC3B2* variant in a heterozygosity similar to the situation in P2. In this cell type, the variant led to decreased *LC3* protein expression, comparable to the knock-down cell line (Fig S3A), and lack of autophagy induction above the UT level in the *LC3B2* c.358 G > A knock-in cell clone (Fig. S3B). Importantly, we observed an increase in expression of VZV *ORF63* DNA (Fig. S3C). These data may suggest that the *LC3B2* variant present in the patient indeed causes less *LC3* expression, potentially disturbing autophagy and resulting in increased VZV replication.

### 3.7 | Patient cells harboring autophagy variants show impaired VZV-induced autophagy, increased VZV transcription and enhanced cell death

Based on the genetic findings, the autophagy induction as well as antiviral immune responses and viability of VZV-infected patient cells was determined. MdMs generated from patients and controls were stimulated with rapamycin, starvation by EBSS incubation or infected with VZV EMC-1. The MdMs of P1 showed a normal LC3-I to LC3-II conversion (Figure 7A,B), whereas P2 cells exhibited reduced levels of LC3-I to LC3-II conversion compared to MdMs from healthy controls (Figure 7C,D). EBSS failed to induce autophagy in MdMs as previously observed. Both patients showed higher transcript levels of VZV *ORF9*, and for P2 also of *ORF63* in PBMCs infected with MeWo-associated VZV rOka compared to healthy controls (Figure 7E,F).

Finally, we examined cell death in response to VZV infection in patient cells, since we previously reported that autophagy defects may enhance virus-induced cytotoxicity and cell death.<sup>73</sup> To this end we performed flow cytometry analysis on different VZV-infected PBMC populations, of which around 10-15% of the monocytes and 5-8% of lymphocytes were infected as measured by gE positive cells by flow cytometry (Fig S4 A). Next, we used Annexin V staining as a reflection of apoptosis (Fig. S4B-D). First, VZV infection of PBMCs led to only a slight increase in Annexin V levels from approximately 75% to 85% (Fig. S4 E, F). When evaluating the T-cell population relevant for VZV infection, we found that Annexin V staining was enhanced in P2 compared to controls in both unstimulated cells as well as in staurosporine and VZV-infected cells. For P1 Annexin V levels were similar between patient and control T-cells (Figure 7G and Fig. S4C). B-cells of both patients showed increased cell death in UT conditions and upon staurosporine treatment, but no difference in VZV-infected samples (Figure 7H and Fig S4 D). In the monocytic fractions there was no major difference between patients and controls, except for a slightly reduced Annexin V staining in P1 compared to controls in the mock (Fig. S4E,F).

## 4 | DISCUSSION

In this study we demonstrate that autophagy is activated during VZV infection in cells of neuronal origin and that autophagy exerts an antiviral role against VZV in these cell types. We further characterize the cellular and viral requirements for this phenomenon. More specifically, we demonstrate that VZV-induced autophagy depends

**FIGURE 5** Co-localization of varicella zoster virus glycoprotein E and p62 in autophagy defective SH-SY5Y cells. (A-D) Immunofluorescence images of SH-SY5Y AAVS1 KD (A), *ULK1* KD (B), *LC3B2* (C) or *ATG5* KD (D), cells stained for VZV glycoprotein (g) E (red), *LC3* (green), p62 (magenta) and DAPI (blue) uninfected or following 48 h infection with VZV EMC-1 MOI = 1. Scale bar = 50  $\mu$ m. Pictures are representative for 5 images per conditions each. The box area is enlarged and shown for merged, p62 and gE. (E) Quantification of mean fluorescent intensity (MFI) of p62 in UT or VZV infected cells. (F) Pearson's correlation coefficients of VZV-infected SH-SY5Y cells. Shown are individual data points plus mean  $\pm$  SD, statistics calculated using two-way ANOVA with Šidák's multiple comparison, \* =  $p < 0.05$ , ns = nonsignificant.

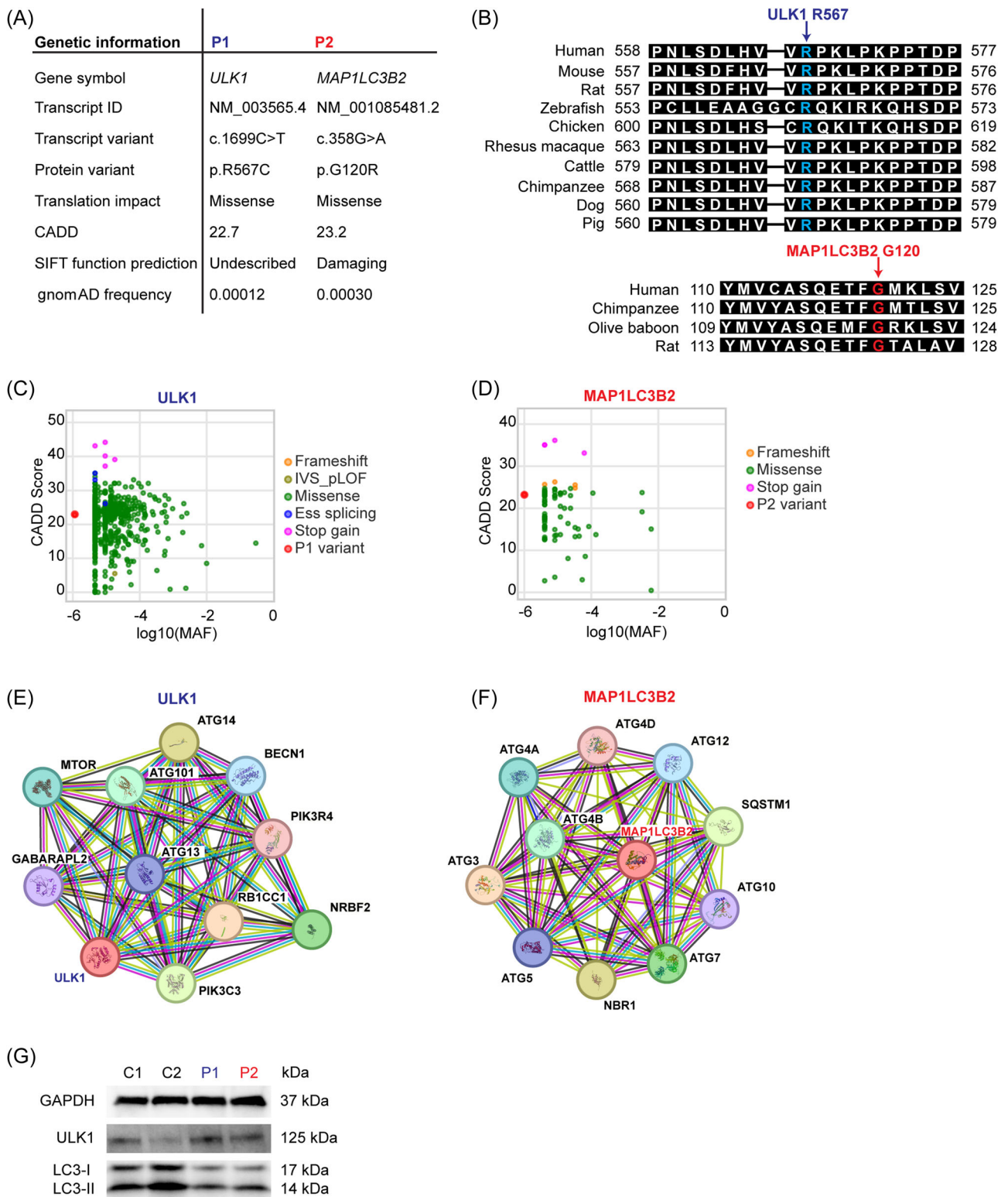


**FIGURE 6** Identification of potentially disease causing variants in *ULK1* and *MAP1LC3B2* in patients with varicella zoster virus CNS infection. (A) Summary of genetic characteristics of the identified *ULK1* R567C and *LC3B2* G120R variants. (B) Alignment of the protein sequence around the identified patient variants in several species for *ULK1* (top) and *LC3B2* (bottom). (C, D) PopViz plot for variants reported for (C) *ULK1* and (D) *MAP1LC3B2*, displaying annotation dependent depletion (CADD) score over minor allele frequencies (MAF). (E, F) STRING analysis of protein interaction networks for *ULK1* I and *LC3B2*. (G) Immunoblot for basal expression of GAPDH, *ULK1*, *LC3-I*, and *LC3-II* monocyte derived macrophages (Mdm) of P1, P2, and two healthy controls.

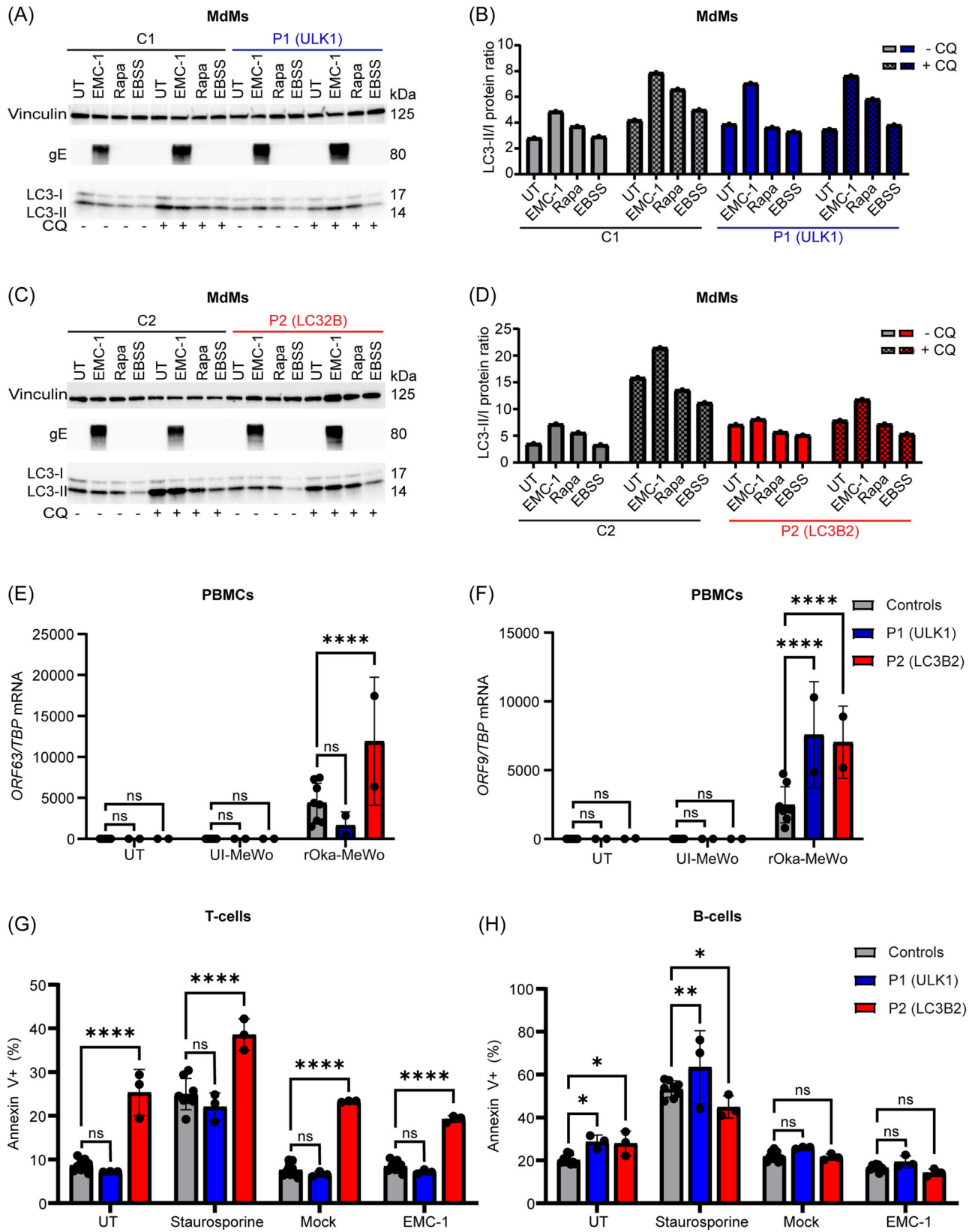


FIGURE 7 (See caption on next page).

on the essential autophagy protein ATG5 and to a lesser extent on other autophagy proteins, including ULK1 and LC3B2. Moreover, the ability of VZV to induce autophagy depends on the integrity of the viral genome and viral replication. We found that autophagy acts in an antiviral manner based on the observations that inducers of autophagy restrict VZV gene transcription and replication and that neuronal cells deficient in the autophagy proteins ATG5, ULK1, and LC3B2 exhibit increased viral replication, with some differences between viral strains. Finally, we provide a link to VZV pathogenesis and clinical infection in humans by identifying potentially disease causing variants in *ULK1* and *MAP1LC3B2* together with decreased autophagy and enhanced VZV replication and cell death in cells from patients with VZV infection in the CNS. Intriguingly, the *LC3B2* 358 G > A variant identified in P2 exerted greater impairment of LC3 expression when introduced in neuroblastoma cells as compared to the patient PBMCs. This might indicate a detrimental effect of the variant somewhat specific to the CNS, which could explain the absence of severe infections outside the CNS in the patient. These data may suggest a deleterious impact of impaired autophagy upon the ability of neurons to restrict and control VZV infection in humans.

Previous studies have demonstrated that induction of autophagy occurs early during the VZV infectious cycle in fibroblasts.<sup>32</sup> Other studies showed detectable LC3-I to LC3-II conversion at 48–72 h postinfection in fibroblasts,<sup>31</sup> in line with our findings. We detected activation of autophagy 72 h postinfection by Western blot analysis on lysates from VZV EMC-1-infected neuron-like cells and slightly earlier at 48 h by immunofluorescence microscopy. In our experimental set-up we did not observe autophagy induction by cell-free VZV rOka isolates in neuroblastoma cells, whereas this has been previously reported for MRC-5 fibroblasts.<sup>32,74</sup> We hypothesize that this is due to a more efficient infection caused by the clinical VZV isolate EMC-1 compared to rOka. In support of this idea, the immunoblots in Figure 1A and C show that infection with VZV EMC-1 leads to higher gE production than VZV rOka infection, despite the MOI used for infection being lower for VZV EMC-1 (MOI 0.1) than for VZV rOka (MOI 0.5). Overall, current literature points towards autophagy as a general response to VZV infection with differences between strains and isolates.<sup>31,75,76</sup> Our results in neuroblastoma cells however indicate that the exact mechanism and role of autophagy might be cell type dependent in VZV infection. As to the viral requirements for activation of autophagy, we found that UV-

inactivated VZV lost the ability to induce autophagy, thereby documenting the essential role of an intact viral genome and viral replication, although we cannot determine whether autophagy is induced by specific viral products or rather reflects general cell stress in the setting of accumulating viral particles during infection. Indeed, the relatively late kinetics of VZV-induced autophagy may suggest the latter mechanism. This hypothesis is supported by previous studies demonstrating VZV-induced autophagy in fibroblasts in connection with ER stress and the unfolded protein response, triggered by accumulation of viral proteins in cells during the course of infection.<sup>75,77</sup> More recently, it was reported that VZV gE facilitates mitophagy to evade STING and MAVS-mediated antiviral innate immunity, also demonstrating the ability of VZV to engage with and activate various autophagic cellular processes.<sup>78</sup>

One important discrepancy between our data obtained in neuronal cells as opposed to previously published results mainly based on VZV infection of fibroblasts and keratinocytes is that autophagy appears antiviral and thereby protective in our experimental cell system. It is a well-documented phenomenon that autophagy may exert either proviral or antiviral roles during infection with different viruses, but also for any given virus in a cell-type and/or time dependent manner.<sup>21,29,79</sup> For example, in the case of HSV-1 infection it was shown that the autophagy blocking viral protein ICP34.5 was crucial for infection of neurons, but dispensable in fibroblasts.<sup>80,81</sup> On the same line, while basal autophagy is required for HSV-2 replication, excessive activation of autophagy may be detrimental to the virus.<sup>80</sup> In an impressive effort, Girsch et al. (2020)<sup>33</sup> established autophagy as a contributing factor to viral egress in VZV-infected fibroblasts, thereby serving in a proviral manner. It is, however, possible that the role of autophagy in neuronal cells may be rather antiviral. Indeed, a large amount of evidence supports a dominantly neuroprotective role of autophagy in several settings, including viral infection.<sup>14,82–85</sup> Additionally, while the autophagic flux induced by VZV was reported to be uninterrupted in skin cells,<sup>76</sup> our data may indicate that late phases of autophagy may be blocked by the virus, further suggesting major differences to the mechanism and outcome of autophagy induction in neuronal cells compared to fibroblasts. Finally, the observed differences in autophagy inducing potential between different VZV strains and the selective effect of autophagy on some but not all VZV ORF transcripts remains unexplained. In particular we don't see any

**FIGURE 7** Decreased autophagy, enhanced viral load and increased apoptosis in patient cells. (A, C) Immunoblots for vinculin, VZV glycoprotein E, LC3-I, and LC3-II in lysates from monocyte-derived macrophages (Mdm) from P1 (A) and P2 (C) and a healthy control, untreated (UT), following 4 h EBSS starvation, 12 h rapamycin (Rapa) stimulation or infection with VZV EMC-1 MOI 0.01 for 48 h. All samples in duplicates +/- chloroquine (CQ). (B, D) Quantification of LC3-II/LC3-I ratios from A, C). Experiment carried out only once due to limited patient material. (E, F) relative expression of the indicated VZV open reading frames (ORF), normalized to the house keeping gene TBP in peripheral blood mononuclear cells (PBMCs) from P1 and P2 and 4 healthy controls after 48 h coculture with uninfected or VZV rOka-infected MeWo cells (1:0.4, PBMC/MeWo). (G, H) Annexin V staining of patient and control PBMCs UT, after 4 h staurosporine treatment or 24 h infection with VZV EMC-1 MOI 0.05. Shown are Annexin V+ T-cells (CD3+ CD19-, G) and B-cells (CD3-CD19+, H). Shown are individual data points plus mean ± SD, statistics were calculated using two-way-ANNOVA with Dunnett's multiple comparison tests, \* =  $p < 0.05$ , \*\* =  $p < 0.01$  \*\*\* =  $p < 0.001$ , \*\*\*\* =  $p < 0.0001$ , ns = nonsignificant.

clear correlation between the ORF affected by autophagy deficiency in relation to kinetic class of ORF, i.e. early, immediate-early or late.

As described above, several single gene IELs, involving defects in type I IFN production or -responses, NK cell number and -function or cellular adaptive immunity have previously been reported to underlie disseminated VZV infection and/or VZV infection in the CNS.<sup>46</sup> Additionally, defects in the autophagy pathway have been proposed as novel IEL predisposing to severe viral disease in recurrent lymphocytic HSV2 Mollaret meningitis,<sup>73</sup> and poliomyelitis.<sup>53</sup> Recently, we reported findings of variants in genes encoding autophagy-molecules in patients suffering from severe disease following VZV infection or -reactivation, including VZV encephalitis and VZV-induced ARN.<sup>47,48</sup> Here, we show reduced, but not abolished, autophagy in MdMs together with increased VZV replication in PBMCs from two patients with VZV CNS infection harboring variants in *ULK1* and *MAP1LC3B2*. Interestingly, a different *MAP1LC3B2* variant was identified in a previous study in a patient with Mollarets meningitis.<sup>73</sup> The reason, why the observed autophagy defect is only partial, may be due to the fundamental, evolutionarily conserved importance of a functional autophagy process in maintaining cellular homeostasis. A complete deficiency in autophagy has not been described in humans and would most likely be lethal, as also evidenced by data from mouse autophagy knock-out studies.<sup>86</sup> Patient PBMCs further show increased VZV replication, and for P2 also increased apoptotic cell death compared to controls. These results indicate that despite some remaining capacity of patient cells to undergo LC3-I to LC3-II conversion, the partial defect is interfering with viral control and protection from cell death. Autophagy has previously been described as a regulator of apoptosis,<sup>26</sup> and accordingly failure to maintain tightly regulated apoptosis in infected cells may contribute to the pathogenesis and serious disease phenotypes by accelerating cell death. Hence, we postulate that IELs in autophagy-related genes may specifically enhance susceptibility to severe CNS infection with VZV.

A limitation of the present study is the lack of neuronal cells from patients. In the same way, our findings on autophagy induction by VZV and enhanced viral replication in states of autophagy defect should be further explored in additional neuronal cell types relevant for VZV CNS infection, such as neuronal LUHMES cells or induced pluripotent stem cells (iPSC)-derived neurons. In addition, vascular endothelial cell models may provide important information, given that VZV neuroinfection can affect blood vessels, with CNS vasculitis and stroke contributing to pathology and neuronal damage in some patients with very severe or fatal outcome of infection.<sup>42,87</sup> Moreover, it would be interesting and relevant to utilize an experimental system that more precisely reflects the situation in a given patient by introducing the specific patient variant into a neuronal cell line or by obtaining patient-derived neurons from differentiated pluripotent stem cells/neuronal iPSCs.

Finally, it should be noted that due to the age of these patients, we assume their complications have arisen following VZV reactivation from latency in sensory ganglia. Given that these patients had an uneventful disease course during primary infection

this may indicate a failure to control virus latency rather than primary VZV replication during primary infection. Our model system on the other hand reflects a situation of lytic virus infection and it would therefore be interesting to study a cellular infection model more directly reflecting VZV latency and reactivation. This is of particular interest, because autophagy has been described as a mode to control apoptosis in herpesvirus latency.<sup>26</sup> Collectively, many questions regarding the mechanism of autophagy activation and the consequences hereof in VZV-infected neuronal cells remain unanswered and will require a multitude of further experimental models and approaches.

## 5 | CONCLUSION

In conclusion, we report a novel antiviral function of autophagy in VZV-infected neuronal cells. The activation of autophagy in neuronal cells requires replicating virus and small-molecule-mediated activation of autophagy exerts strong antiviral activity. Failure to produce a sufficient autophagic response, due to impaired function of autophagy proteins ATG5, ULK1 and LC3B2 in neuronal cell models or in PBMCs/MdMs from patients with genetic defects in autophagy-related genes, causes increased viral titers and increased T-cell apoptotic death, and thereby represents IELs related to autophagy specifically increasing the susceptibility to VZV neuroinfection. This work continues our efforts to elucidate the pathogenesis of VZV neuroinfection and demonstrates a previously underestimated role for autophagy in neuroprotection from VZV in humans. Finally, the data suggest that IEL in autophagy pathways should be sought in patients with severe VZV neuroinfection, and further point to a new direction for development of improved options for prophylaxis and treatment to alleviate severe outcomes and complications of VZV neuroinfection.

## AUTHOR CONTRIBUTIONS

THM conceived the idea; THM, GMGMV, AG, MMT, JLH and JvH cared for patients and/or collected and isolated patient and biological material; JLH, DMH, MM, JW, FR, IKDS, LH, and TZ performed experiments and analyzed data together with SRP, AVB, VSS, and THM. JLH and THM wrote the first draft of the manuscript, THM coordinated and wrote the revised manuscript, all authors contributed, read, commented and approved the final version of the manuscript.

## ACKNOWLEDGMENTS

We wish to thank the patients participating in this study. In addition, we are grateful to Bettina Bundgaard for excellent technical assistance. Flow cytometry experiments were performed at and with outstanding technical guidance from the FACS Core Facility, Aarhus University, Denmark. Likewise, immunofluorescence images were acquired at and with outstanding technical guidance from the Facility for Imaging by Light Microscopy at Imperial College London. THM was funded by The Independent Research Fund Denmark (4004-00047B), Danish

National Research Foundation (DNRF164), The Lundbeck Foundation (R268–3927), NOVO Nordisk Research Foundation, Distinguished clinical investigator (NNF21OC0067157, NNF20OC0063436), Deutsche Forschungsgemeinschaft (390874280), and JLH received support from Danielsen's Fond.

### CONFLICT OF INTEREST STATEMENT

The authors declare no conflict of interest.

### DATA AVAILABILITY STATEMENT

The data that support the findings of this study are available on request from the corresponding author. The data are not publicly available due to privacy or ethical restrictions. The data from this study can be shared upon request, according to national and international General Data Protection Regulation rules and following individual Data Transfer Agreement and Material Transfer Agreement rules. Relevant data can be shared to researchers upon request to the corresponding author.

### ETHICS STATEMENT

Patients were included following oral and written consent, in accordance with The Helsinki Declaration, the Data Protection Agency, Institutional Review Board and the Swedish Ethical Review Authority (P1: no. 2019-02544, P2: no. 2020-04850).

### ORCID

Abel Viejo-Borbolla  <http://orcid.org/0000-0001-6395-4010>

### REFERENCES

- de Duve C. The lysosome. *Sci Am*. 1963;208:64-73. doi:10.1038/scientificamerican0563-64
- de Duve C, Wattiaux R. Functions of lysosomes. *Annu Rev Physiol*. 1966;28:435-492. doi:10.1146/annurev.ph.28.030166.002251
- Mizushima N. A brief history of autophagy from cell biology to physiology and disease. *Nature Cell Biol*. 2018;20(5):521-527. doi:10.1038/s41556-018-0092-5
- Ichimura Y, Kirisako T, Takao T, et al. A ubiquitin-like system mediates protein lipidation. *Nature*. 2000;408(6811):488-492. doi:10.1038/35044114
- Mizushima N, Noda T, Yoshimori T, et al. A protein conjugation system essential for autophagy. *Nature*. 1998;395(6700):395-398. doi:10.1038/26506
- Popelka H, Klionsky DJ. Autophagic structures revealed by cryo-electron tomography: new clues about autophagosome biogenesis. *Autophagy*. 2023;19(5):1375-1377. doi:10.1080/15548627.2023.2175305
- Wu Z, Zhou C, Que H, Wang Y, Rong Y. The fate of autophagosomal membrane components. *Autophagy*. 2023;19(1):370-371. doi:10.1080/15548627.2022.2083807
- Ericsson JLE. Studies on induced cellular autophagy. *Exp Cell Res*. 1969;55(1):95-106. doi:10.1016/0014-4827(69)90462-5
- Klionsky DJ, Abdel-Aziz AK, Abdelfatah S, et al. Guidelines for the use and interpretation of assays for monitoring autophagy (4th edition)1. *Autophagy*. 2021;17(1):1-382. doi:10.1080/15548627.2020.1797280
- Berg TO, Fengsrud M, Strømhaug PE, Berg T, Seglen PO. Isolation and characterization of rat liver amphisomes. *J Biol Chem*. 1998;273(34):21883-21892. doi:10.1074/jbc.273.34.21883
- Gordon PB, Seglen PO. Prelysosomal convergence of autophagic and endocytic pathways. *Biochem Biophys Res Commun*. 1988;151(1):40-47. doi:10.1016/0006-291x(88)90556-6
- Szatmári Z, Kis V, Lippai M, et al. Rab11 facilitates cross-talk between autophagy and endosomal pathway through regulation of hook localization. *Mol Biol Cell*. 2014;25(4):522-531. doi:10.1091/mbc.E13-10-0574
- Takahashi S, Kubo K, Waguri S, et al. Rab11 regulates exocytosis of recycling vesicles at the plasma membrane. *J Cell Sci*. 2012;125(Pt 17):4049-4057. doi:10.1242/jcs.102913
- Levine B, Kroemer G. Biological functions of autophagy genes: A disease perspective. *Cell*. 2019;176(1-2):11-42. doi:10.1016/j.cell.2018.09.048
- Levine B, Kroemer G. Autophagy in the pathogenesis of disease. *Cell*. 2008;132(1):27-42. doi:10.1016/j.cell.2007.12.018
- Shintani T, Klionsky DJ. Autophagy in health and disease: a double-edged sword. *Science*. 2004;306(5698):990-995. doi:10.1126/science.1099993
- Mizushima N, Levine B, Cuervo AM, Klionsky DJ. Autophagy fights disease through cellular self-digestion. *Nature*. 2008;451(7182):1069-1075. doi:10.1038/nature06639
- Chen M, Hong MJ, Sun H, et al. Essential role for autophagy in the maintenance of immunological memory against influenza infection. *Nature Med*. 2014;20(5):503-510. doi:10.1038/nm.3521
- de Lichtenberg U, Jensen LJ, Brunak S, Bork P. Dynamic complex formation during the yeast cell cycle. *Science*. 2005;307(5710):724-727. doi:10.1126/science.1105103
- Gutierrez MG, Master SS, Singh SB, Taylor GA, Colombo MI, Deretic V. Autophagy is a defense mechanism inhibiting BCG and mycobacterium tuberculosis survival in infected macrophages. *Cell*. 2004;119(6):753-766. doi:10.1016/j.cell.2004.11.038
- Choi Y, Bowman JW, Jung JU. Autophagy during viral infection - a double-edged sword. *Nat Rev Microbiol*. 2018;16(6):341-354. doi:10.1038/s41579-018-0003-6
- Cavignac Y, Esclatine A. Herpesviruses and autophagy: catch me if you can. *Viruses*. 2010;2(1):314-333. doi:10.3390/v2010314
- Nakahira K, Haspel JA, Rathinam VAK, et al. Autophagy proteins regulate innate immune responses by inhibiting the release of mitochondrial DNA mediated by the NALP3 inflammasome. *Nature Immunol*. 2011;12(3):222-230. doi:10.1038/ni.1980
- Prabakaran T, Bodda C, Krapp C, et al. Attenuation of cGAS-STING signaling is mediated by a p62/SQSTM1-dependent autophagy pathway activated by TBK1. *EMBO J*. 2018;37(8):e97858. doi:10.15252/embj.201797858
- Tal MC, Sasai M, Lee HK, Yordy B, Shadel GS, Iwasaki A. Absence of autophagy results in reactive oxygen species-dependent amplification of RLR signaling. *Proceedings of the National Academy of Sciences*. 2009;106(8):2770-2775. doi:10.1073/pnas.0807694106
- Lussignol M, Esclatine A. Herpesvirus and autophagy: "all right, everybody be cool, this is a robbery!". *Viruses*. 2017;9(12):372. doi:10.3390/v9120372
- Kirkegaard K. Subversion of the cellular autophagy pathway by viruses. *Curr Top Microbiol Immunol*. 2009;335:323-333. doi:10.1007/978-3-642-00302-8\_16
- Jackson WT, Giddings TH, Taylor MP, et al. Subversion of cellular autophagosomal machinery by RNA viruses. *PLoS Biol*. 2005;3(5):e156. doi:10.1371/journal.pbio.0030156
- Sir D, Chen W, Choi J, Wakita T, Yen TSB, Ou HJ. Induction of incomplete autophagic response by hepatitis C virus via the unfolded protein response. *Hepatology*. 2008;48(4):1054-1061. doi:10.1002/hep.22464
- Dreux M, Gastaminza P, Wieland SF, Chisari FV. The autophagy machinery is required to initiate hepatitis C virus replication. *Proceedings of the National Academy of Sciences*. 2009;106(33):14046-14051. doi:10.1073/pnas.0907344106



31. Takahashi M, Jackson W, Laird DT, et al. Varicella-zoster virus infection induces autophagy in both cultured cells and human skin vesicles. *J Virol.* 2009;83(11):5466-5476. doi:10.1128/JVI.02670-08
32. Buckingham EM, Carpenter JE, Jackson W, Grose C. Autophagy and the effects of its inhibition on varicella-zoster virus glycoprotein biosynthesis and infectivity. *J Virol.* 2014;88(2):890-902. doi:10.1128/JVI.02646-13
33. Girsch JH, Jackson W, Carpenter JE, Moninger TO, Jarosinski KW, Grose C. Exocytosis of progeny infectious Varicella-Zoster virus particles via a Mannose-6-Phosphate receptor pathway without xenophagy following secondary envelopment. *J Virol.* 2020;94(16):e00800-20. doi:10.1128/JVI.00800-20
34. Gershon AA, Breuer J, Cohen JL, et al. Varicella zoster virus infection. *Nat Rev Dis Primers.* 2015;1:15016. doi:10.1038/nrdp.2015.16
35. Kennedy PGE, Grinfeld E, Gow JW. Latent varicella-zoster virus is located predominantly in neurons in human trigeminal ganglia. *Proceedings of the National Academy of Sciences.* 1998;95(8):4658-4662. doi:10.1073/pnas.95.8.4658
36. Rovnak J, Kennedy PGE, Badani H, Cohrs RJ. A comparison of herpes simplex virus type 1 and varicella-zoster virus latency and reactivation. *J Gen Virol.* 2015;96(Pt 7):1581-1602. doi:10.1099/vir.0.000128
37. Kennedy P, Gershon A. Clinical features of Varicella-Zoster virus infection. *Viruses.* 2018;10(11):609. doi:10.3390/v10110609
38. Nagel MA, Gilden DH. The protean neurologic manifestations of varicella-zoster virus infection. *Cleve Clin J Med.* 2007;74(7):489-494. doi:10.3949/ccjm.74.7.489
39. Kennedy PGE. The spectrum of neurological manifestations of Varicella-Zoster virus reactivation. *Viruses.* 2023;15(8):1663. doi:10.3390/v15081663
40. Grahn A, Studahl M. Varicella-zoster virus infections of the central nervous system - prognosis, diagnostics and treatment. *J Infect.* 2015;71(3):281-293. doi:10.1016/j.jinf.2015.06.004
41. Muthiah MN, Michaelides M, Child CS, Mitchell SM. Acute retinal necrosis: a national population-based study to assess the incidence, methods of diagnosis, treatment strategies and outcomes in the UK. *Br J Ophthalmol.* 2007;91(11):1452-1455. doi:10.1136/bjo.2007.114884
42. Kleinschmidt-DeMasters BK, Gilden DH. Varicella-Zoster virus infections of the nervous system. *Arch Pathol Lab Med.* 2001;125(6):770-780. doi:10.5858/2001-125-0770-VZVIOT
43. Iwahashi-Shima C, Azumi A, Ohguro N, et al. Acute retinal necrosis: factors associated with anatomic and visual outcomes. *Jpn J Ophthalmol.* 2013;57(1):98-103. doi:10.1007/s10384-012-0211-y
44. Herlin LK, Hansen KS, Bodilsen J, et al. Varicella zoster virus encephalitis in Denmark from 2015 to 2019-A nationwide prospective cohort study. *Clin Infect Dis.* 2021;72(7):1192-1199. doi:10.1093/cid/ciaa185
45. Kennedy PG, Mogensen TH. Determinants of neurological syndromes caused by varicella zoster virus (VZV). *J Neurovirol.* 2020;26(4):482-495. doi:10.1007/s13365-020-00857-w
46. Jouanguy E, Béziat V, Mogensen TH, Casanova J-L, Tangye SG, Zhang S-Y. Human inborn errors of immunity to herpes viruses. *Curr Opin Immunol.* 2020;62:106-122. doi:10.1016/j.coi.2020.01.004
47. Thomsen MM, Tyrberg T, Skaalum K, et al. Genetic variants and immune responses in a cohort of patients with varicella zoster virus encephalitis. *J Infect Dis.* 2021;224(12):2122-2132. doi:10.1093/infdis/jiab254
48. Heinz JL, Swagemakers SMA, von Hofsten J, et al. Whole exome sequencing of patients with varicella-zoster virus and herpes simplex virus induced acute retinal necrosis reveals rare disease-associated genetic variants. *Front Mol Neurosci.* 2023;16:1253040. doi:10.3389/fnmol.2023.1253040
49. Kircher M, Witten DM, Jain P, O'Roak BJ, Cooper GM, Shendure J. A general framework for estimating the relative pathogenicity of human genetic variants. *Nature Genet.* 2014;46(3):310-315. doi:10.1038/ng.2892
50. Itan Y, Shang L, Boisson B, et al. The mutation significance cutoff: gene-level thresholds for variant predictions. *Nature Methods.* 2016;13(2):109-110. doi:10.1038/nmeth.3739
51. Szklarczyk D, Franceschini A, Wyder S, et al. STRING v10: protein-protein interaction networks, integrated over the tree of life. *Nucleic Acids Res.* 2015;43(Database issue):D447-D452. doi:10.1093/nar/gku1003
52. Zhang P, Bigio B, Rapaport F, et al. PopViz: a webserver for visualizing minor allele frequencies and damage prediction scores of human genetic variations. *Bioinformatics.* 2018;34(24):4307-4309. doi:10.1093/bioinformatics/bty536
53. Brinck Andersen N-S, Jørgensen SE, Skipper KA, et al. Essential role of autophagy in restricting poliovirus infection revealed by identification of an ATG7 defect in a poliomyelitis patient. *Autophagy.* 2021;17(9):2449-2464. doi:10.1080/15548627.2020.1831800
54. Sloutskin A, Goldstein RS. Laboratory preparation of Varicella-Zoster virus: concentration of virus-containing supernatant, use of a debris fraction and magnetofection for consistent cell-free VZV infections. *J Virol Methods.* 2014;206:128-132. doi:10.1016/j.jviromet.2014.05.027
55. Farahani E, Reinert LS, Narita R, et al. The HIF transcription network exerts innate antiviral activity in neurons and limits brain inflammation. *Cell Rep.* 2024;43(2):113792. doi:10.1016/j.celrep.2024.113792
56. Christensen J, Steain M, Slobedman B, Abendroth A. Differentiated neuroblastoma cells provide a highly efficient model for studies of productive varicella-zoster virus infection of neuronal cells. *J Virol.* 2011;85(16):8436-8442. doi:10.1128/JVI.00515-11
57. Maimaitili M, Chen M, Febbraro F, et al. Enhanced production of mesencephalic dopaminergic neurons from lineage-restricted human undifferentiated stem cells. *Nat Commun.* 2023;14(1):7871. doi:10.1038/s41467-023-43471-0
58. Andersen LL, Mørk N, Reinert LS, et al. Functional IRF3 deficiency in a patient with herpes simplex encephalitis. *J Exp Med.* 2015;212(9):1371-1379. doi:10.1084/jem.20142274
59. Stirling DR, Swain-Bowden MJ, Lucas AM, Carpenter AE, Cimini BA, Goodman A. CellProfiler 4: improvements in speed, utility and usability. *BMC Bioinformatics.* 2021;22(1):433. doi:10.1186/s12859-021-04344-9
60. Taft J, Markson M, Legarda D, et al. Human TBK1 deficiency leads to autoinflammation driven by TNF-induced cell death. *Cell.* 2021;184(17):4447-4463.e20. doi:10.1016/j.cell.2021.07.026
61. Schneider CA, Rasband WS, Eliceiri KW. NIH image to ImageJ: 25 years of image analysis. *Nature Methods.* 2012;9(7):671-675. doi:10.1038/nmeth.2089
62. Bolte S, Cordelières FP. A guided tour into subcellular colocalization analysis in light microscopy. *J Microsc.* 2006;224(Pt 3):213-232. doi:10.1111/j.1365-2818.2006.01706.x
63. Beránková Z, Kopecký J, Kobayashi S, Lieskovská J. Dual control of tick-borne encephalitis virus replication by autophagy in mouse macrophages. *Virus Res.* 2022;315:198778. doi:10.1016/j.virusres.2022.198778
64. Kennedy JJ, Steain M, Slobedman B, Abendroth A. Infection and functional modulation of human monocytes and macrophages by Varicella-Zoster virus. *J Virol.* 2019;93(3):e01887-18. doi:10.1128/JVI.01887-18
65. Dunn KW, Kamočka MM, McDonald JH. A practical guide to evaluating colocalization in biological microscopy. *American Journal of Physiology-Cell Physiology.* 2011;300(4):C723-C742. doi:10.1152/ajpcell.00462.2010
66. Manders EMM, Verbeek FJ, Aten JA. Measurement of colocalization of objects in dual-colour confocal images. *J Microsc.* 1993;169(3):375-382. doi:10.1111/j.1365-2818.1993.tb03313.x

67. Azarkh Y, Dölken L, Nagel M, Gildden D, Cohrs RJ. Synthesis and decay of varicella zoster virus transcripts. *J Neurovirol.* 2011;17(3):281-287. doi:10.1007/s13365-011-0029-2
68. Braspenning SE, Sadaoka T, Breuer J, Verjans GMGM, Ouwendijk WJD, Depledge DP. Decoding the architecture of the Varicella-Zoster virus transcriptome. *mBio.* 2020;11(5):e01568-20. doi:10.1128/mBio.01568-20
69. Inoue N, Matsushita M, Fukui Y, et al. Identification of a varicella-zoster virus replication inhibitor that blocks capsid assembly by interacting with the floor domain of the major capsid protein. *J Virol.* 2012;86(22):12198-12207. doi:10.1128/JVI.01280-12
70. Baiker A, Bagowski C, Ito H, et al. The immediate-early 63 protein of Varicella-Zoster virus: analysis of functional domains required for replication in vitro and for t-cell and skin tropism in the SCIDhu model in vivo. *J Virol.* 2004;78(3):1181-1194. doi:10.1128/jvi.78.3.1181-1194.2004
71. Abendroth A, Morrow G, Cunningham AL, Slobedman B. Varicella-zoster virus infection of human dendritic cells and transmission to T cells: implications for virus dissemination in the host. *J Virol.* 2001;75(13):6183-6192. doi:10.1128/JVI.75.13.6183-6192.2001
72. Zachari M, Ganley IG. The mammalian ULK1 complex and autophagy initiation. *Essays Biochem.* 2017;61(6):585-596. doi:10.1042/EBC20170021
73. Hait AS, Olanier D, Sancho-Shimizu V, et al. Defects in LC3B2 and ATG4A underlie HSV2 meningitis and reveal a critical role for autophagy in antiviral defense in humans. *Science Immunology.* 2020;5(54):eabc2691. doi:10.1126/sciimmunol.abc2691
74. Graybill C, Morgan MJ, Levin MJ, Lee KS. Varicella-zoster virus inhibits autophagosome-lysosome fusion and the degradation stage of mTOR-mediated autophagic flux. *Virology.* 2018;522:220-227. doi:10.1016/j.virol.2018.07.018
75. Carpenter JE, Jackson W, Benetti L, Grose C. Autophagosome formation during varicella-zoster virus infection following endoplasmic reticulum stress and the unfolded protein response. *J Virol.* 2011;85(18):9414-9424. doi:10.1128/JVI.00281-11
76. Buckingham EM, Carpenter JE, Jackson W, Zerboni L, Arvin AM, Grose C. Autophagic flux without a block differentiates varicella-zoster virus infection from herpes simplex virus infection. *Proceedings of the National Academy of Sciences.* 2015;112(1):256-261. doi:10.1073/pnas.1417878112
77. Carpenter JE, Grose C. Varicella-zoster virus glycoprotein expression differentially induces the unfolded protein response in infected cells. *Front Microbiol.* 2014;5:322. doi:10.3389/fmicb.2014.00322
78. Oh S-J, Yu J-W, Ahn J-H, et al. Varicella zoster virus glycoprotein E facilitates PINK1/Parkin-mediated mitophagy to evade STING and MAVS-mediated antiviral innate immunity. *Cell Death Dis.* 2024;15(1):16. doi:10.1038/s41419-023-06400-z
79. Lennemann NJ, Coyne CB. Catch me if you can: the link between autophagy and viruses. *PLoS Pathog.* 2015;11(3):e1004685. doi:10.1371/journal.ppat.1004685
80. Alexander DE, Ward SL, Mizushima N, Levine B, Leib DA. Analysis of the role of autophagy in replication of herpes simplex virus in cell culture. *J Virol.* 2007;81(22):12128-12134. doi:10.1128/JVI.01356-07
81. Yordy B, Iijima N, Huttner A, Leib D, Iwasaki A. A neuron-specific role for autophagy in antiviral defense against herpes simplex virus. *Cell Host Microbe.* 2012;12(3):334-345. doi:10.1016/j.chom.2012.07.013
82. Stavoe AKH, Holzbaur ELF. Axonal autophagy: mini-review for autophagy in the CNS. *Neurosci Lett.* 2019;697:17-23. doi:10.1016/j.neulet.2018.03.025
83. Gonzalez Porras MA, Sieck GC, Mantilla CB. Impaired autophagy in motor neurons: a final common mechanism of injury and death. *Physiology.* 2018;33(3):211-224. doi:10.1152/physiol.00008.2018
84. Borsa M, Obba S, Richter FC, et al. Autophagy preserves hematopoietic stem cells by restraining mTORC1-mediated cellular anabolism. *Autophagy.* 2023;20:45-57. doi:10.1080/15548627.2023.2247310
85. Lewerissa EI, Nadif Kasri N, Linda K. Epigenetic regulation of autophagy-related genes: implications for neurodevelopmental disorders. *Autophagy.* 2023;20:15-28. doi:10.1080/15548627.2023.2250217
86. Kuma A, Hatano M, Matsui M, et al. The role of autophagy during the early neonatal starvation period. *Nature.* 2004;432(7020):1032-1036. doi:10.1038/nature03029
87. Gildden D, Cohrs RJ, Mahalingam R, Nagel MA. Varicella zoster virus vasculopathies: diverse clinical manifestations, laboratory features, pathogenesis, and treatment. *Lancet Neurol.* 2009;8(8):731-740. doi:10.1016/S1474-4422(09)70134-6

## SUPPORTING INFORMATION

Additional supporting information can be found online in the Supporting Information section at the end of this article.

**How to cite this article:** Heinz JL, Hinke DM, Maimaitili M, et al. Varicella zoster virus-induced autophagy in human neuronal and hematopoietic cells exerts antiviral activity. *J Med Virol.* 2024;96:e29690. doi:10.1002/jmv.29690